



Cite this: *Mater. Adv.*, 2024, 5, 394

Received 30th October 2023,  
Accepted 30th November 2023

DOI: 10.1039/d3ma00924f

rsc.li/materials-advances

## Layered nanomaterials for renewable energy generation and storage

Anna A. Nikitina,<sup>a</sup> Filipp V. Lavrentev,<sup>a</sup> Veronika Yu. Yurova,<sup>a</sup> Daniil Yu. Piarnits,<sup>a</sup> Olga O. Volkova,<sup>a</sup> Ekaterina V. Skorb<sup>ID \*</sup><sup>a</sup> and Dmitry G. Shchukin<sup>ID \*</sup><sup>b</sup>

This study focuses on potential applications of two-dimensional (2D) materials in renewable energy research. Additionally, we briefly discuss other implementations of 2D materials in smart systems like self-healing coatings and electrochemical reduction of carbon dioxide and nitrogen. We highlight the recent advancements in energy storage technology, phase change materials, materials' fundamental characteristics, and summarise perspectives of their future applications in energy technology and related fields. Furthermore, we discuss the use of machine learning and big data for optimisation and further development of 2D materials.

### 1. Introduction

Fossil fuels are the main energy sources in human society and account for about 85% of total energy consumption.<sup>1</sup> However, burning fossil fuels led to a gradual depletion of their reserves, which caused an energy crisis and environmental problems.<sup>2-4</sup> Therefore, it is important to search for implementation of renewable energy sources that are sustainable and environmentally friendly. Hydrogen, biofuels, solar, and wind energy are widely used to replace fossil energy sources. One of the main disadvantages of hydrogen energy is that most hydrogen is produced from fossil fuels using well-established technologies such as steam reforming, gasification, and partial oxidation, which are criticised for their high energy consumption and carbon emissions.<sup>5</sup> Biofuels, typically produced through biomass fermentation, have low concentration in the final product and often form mix of liquids with water (azeotropes).<sup>6,7</sup> This can significantly increase production costs and potentially impact the combustion process or pose security concerns during their application. Solar and wind energy disadvantages include production instability depending on the weather conditions and high installation and maintenance costs.<sup>8,9</sup> Therefore, new multi-functional materials are required to solve currents issues of the green energy transition process.

Promising energy harvesting devices can accumulate energy from the environment, allowing for sustainable operation by storing more energy than consumed (Fig. 1).<sup>10</sup> Their advantages have led to significant progress in portable energy harvesting

systems containing 2D materials. First, 2D materials have a large surface to volume ratio, allowing full use of all available active electrode materials.<sup>11</sup> This leads to an increase in contact area between the electrodes and electrolytes and a reduction of the pathway length for charge transfer. Second, atomic-level or nanoscale 2D materials are thin, which makes them flexible and attractive for devices requiring low thickness and high flexibility.<sup>12,13</sup> Moreover, 2D materials have unique properties related to limiting in-plane charge and heat transfer, making them ideal for thermoelectric devices that convert heat into electricity.<sup>14,15</sup> Third, many 2D materials are highly conductive with tunable electronic properties, making them ideal for batteries,<sup>16-18</sup> supercapacitors<sup>19</sup> and other energy storage devices.<sup>20</sup> Remarkable optoelectronic characteristics of these nanomaterials include light emission, optical modulation, saturable adsorption and electrically modulated field effect characteristics, which have contributed to the various LEDs, lasers, optical modulators, photodetectors, and high-performance 2D field-effect transistors.<sup>21-23</sup> The chemical stability of these materials makes it possible to achieve long-term resistance to degradation and corrosion.<sup>24,25</sup> All of these characteristics make 2D materials potential candidates for the next generations of energy storage devices.

In recent years, thin 2D structures with exceptional electrical, optical, thermal and mechanical properties based on graphene and graphene oxide (GO),<sup>26-28</sup> graphyne,<sup>29</sup> graphdiyne (GDY),<sup>30</sup> transition-metal dichalcogenides (TMDs),<sup>31,32</sup> and transition metal carbide, nitride, or carbonitride (MXene),<sup>33,34</sup> and 2D black phosphorus (BP)<sup>35</sup> have demonstrated enormous potential for their applications in various fields of materials science and energy. 2D materials are divided into non-layered and layered materials. Layered 2D materials, unlike non-layered ones, have an isotropic volumetric crystal structure due to covalent bonds and have van der Waals gaps between adjacent layers.<sup>36,37</sup> In particular,

<sup>a</sup> ITMO University, 9, Lomonosova street, Saint Petersburg, 191002, Russia.

E-mail: skorb@itmo.ru

<sup>b</sup> Department of Chemistry, Stephenson Institute for Renewable Energy, University of Liverpool, Liverpool L69 7ZD, UK. E-mail: shchukin@liverpool.ac.uk



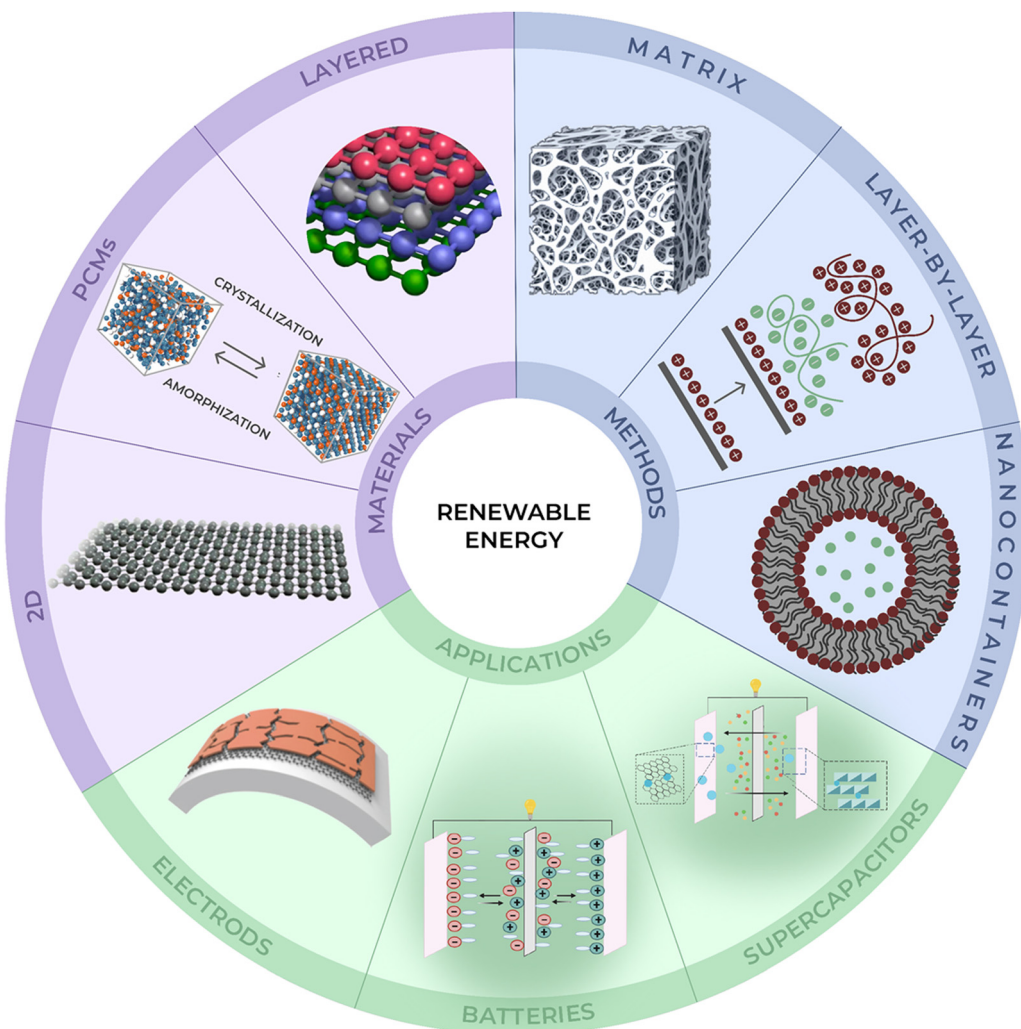


Fig. 1 Schematic illustration of renewable energy materials, methods of their preparation and applications.

van der Waals forces play a significant role in determining the physical properties of substances, such as boiling and melting points, and are important in understanding intermolecular interactions.<sup>38,39</sup>

The use of 2D materials can significantly improve the properties of various types of electronic devices. Due to its high surface area (up to  $2630 \text{ m}^2 \text{ g}^{-1}$ ), electrical conductivity, electron transfer ratio ( $106 \text{ S cm}^{-1}$ ), and modulus of elasticity, graphene has become a leading material in electrochemistry and battery storage.<sup>40,41</sup> Graphdiyne differs from graphene in combining  $\text{sp}^2$ - and  $\text{sp}^3$ -hybridized carbon atoms, while graphene consists of only  $\text{sp}^2$ -hybridized carbon atoms. However, due to the absence of heteroatoms, graphdiyne has low intrinsic electrochemical activity.<sup>42</sup> Therefore, to use graphene in energy storage and conversion, it is necessary to modify it by doping with heteroatoms or hybridise with other active materials. However, graphene cannot be used in high-performance, low-power FET devices due to the low turn-on/off ratios and high turn-off currents that arise from the lack of bandgap.<sup>43</sup>

In turn, some 2D TMDs have the same layered structure features as graphite. Still, most of their bandgap is within 1–2 eV,

and they have strong covalent bonds within layers and weak van der Waals forces between layers, which provide an ideal space for Li intercalation.<sup>44</sup> For batteries, this means better ion intercalation/deintercalation, control of the volumetric expansion of electrode materials and improved lithium storage surface/interface properties. Two-dimensional TMDs can also be used in solar cells to achieve tunable bandgap by adjusting the number of layers and ensure more efficient absorption of sunlight as compared to conventional materials like silicon or gallium arsenide.<sup>45,46</sup> 2D TMDs have a direct bandgap – leading to efficient charge separation and collection. Therefore, by controlling the thickness of the TMDs, their bandgap can be tailored to match most of the solar spectrum, allowing for more efficient absorption of sunlight.<sup>47</sup> Moreover, TMDs have demonstrated multiple light-matter solid reflections, which means they can absorb a significant amount of light even in ultrathin layers.<sup>48</sup>

Using the unique MXenes structure for supercapacitors can provide a fast electron supply due to their individual conductive transition metal carbide layers, which have efficient electron transport.<sup>49</sup> This enables increased charge storage and fast

charging/discharging rates in supercapacitors through their versatile surface terminal groups, which act as active centres for rapid redox reactions.<sup>50</sup> MXenes have high proton availability due to their hydrophilic surface terminal groups.

The unique puckered monolayer geometry gives 2D black phosphorus or phosphorene many unprecedented properties, making it a promising electrode material for electrochemical energy storage devices, such as lithium-ion batteries, supercapacitors, and emerging technologies like lithium–sulfur batteries, magnesium-ion batteries and sodium-ion batteries.<sup>51</sup> The intrinsic in-plane anisotropy and moderate bandgap of phosphorene have stimulated considerable efforts in developing its potential in thermoelectric applications due to the large Seebeck coefficient and high carrier mobility. The phosphorene bandgap can be tuned from 0.3 to 2 eV by decreasing its thickness from bulk to single layer. Such an adjustment can be engineered by the plane strain and edge structures providing more flexibility in device design.<sup>52,53</sup> It is important to note that, despite promising properties, phosphorene has challenges such as low yield in preparation and poor air stability.

This review summarises recent advances in 2D materials for energy sources, methods for the layered structures fromation, and applications of phase transition materials (PCMs) for thermal energy storage. We focus on using machine learning (ML) as a versatile and effective tool to predict the structural, electronic, mechanical, and chemical properties of 2D materials that have yet to be discovered.

## 2. Methods for the formation of layered structures

The development of functional micro- and nanocontainers is of great interest in various research and application areas, including biotechnology,<sup>54,55</sup> medicine,<sup>56,57</sup> cosmetics,<sup>58,59</sup> catalysis,<sup>60,61</sup> and the creation of multifunctional materials.<sup>62,63</sup> Nanocontainers have a unique ability to isolate active substances from the surrounding environment and release them as needed. To achieve this goal, stable shell structures of nanocontainers should be designed to possess the required functionalities and enable the controlled release of active substances. Various external stimuli and methods can be used for this purpose, including changes in pH,<sup>64</sup> temperature,<sup>65</sup> magnetic fields,<sup>66</sup> light irradiation.<sup>67,68</sup>

Currently, the following approaches for creating “smart” materials have gained wide popularity.<sup>69,70</sup> The first approach is based on the self-assembly of lipid molecules or amphiphilic block copolymers into spherical bilayer structures known as vesicles.<sup>71,72</sup> The second approach involves using dendrimers or hyperbranched polymers as nanocontainers.<sup>73,74</sup> The third one includes suspension and emulsion polymerisation around nanodroplets of oil or water, forming a polymer shell around them. This method can be enhanced using ultrasound and allows for the creating of hollow nanostructures with a size of approximately 20 nm.<sup>75</sup> It represents a simple one-step process and has been widely studied, with several reviews dedicated to the emulsion polymerisation technique.<sup>71,75,76</sup> Inorganic frameworks

of nanocontainers, such as mesoporous silica or nanotubes made of titanium dioxide and gallium zeolite equipped with nanogates with adjustable pores, exhibit higher mechanical strength and are more cost-effective comparing to polymer nanocontainers.<sup>77–79</sup>

### 2.1. Layer-by-layer method – protective coatings

Layer-by-layer (LbL) assembly has become a helpful tool for creating functional nanofilms with various applications.<sup>80,81</sup> This universal method enables the fabrication of thin films on the surfaces of various shapes. One of the key benefits of LbL is the ability to tailor the chemical nature of the surface, making it flexible and adaptive.<sup>82–84</sup> Additionally, LbL draws inspiration from processes occurring in living organisms, allowing the creation of biomimetic materials. The LbL method has been automated and is now used to develop new commercial products.<sup>85,86</sup> Industry explores future directions for applying LbL, such as functional coatings on complex surfaces,<sup>87–90</sup> membranes<sup>81,91,92</sup> and material design,<sup>93,94</sup> and for biomedical delivery applications.<sup>95–97</sup>

One of the most developed examples of LbL assembly application is fabrication of protective coatings, including anticorrosion and anti-graffiti coatings.<sup>98,99</sup> Significant developments in this field include films that inhibit corrosion processes on metal surfaces and use of nanocarriers to store and release corrosion inhibitors. LbL assembly enables the development of intelligent coatings that can adapt to environmental changes and repair themselves if damaged.<sup>100</sup>

Shechukin *et al.* was the first to apply the LbL assembly method to deposit polystyrene sulfonate (PSS) polyelectrolyte multilayer films onto the surface of halloysite nanotubes, which were preloaded with corrosion inhibitors.<sup>101</sup> After incorporating these halloysite nanocarriers into composite  $\text{SiO}_x/\text{ZrO}_y$  sol-gel coatings, the composite coatings demonstrated effective corrosion protection of aluminium over an extended period up to 10 years. Multilayer composite LbL films enable efficient storage of inhibitors and their long-term release (Fig. 2).

Similarly,  $\text{SiO}_2$  particles coated with LbL multilayer films containing inhibitors were used as nanocarriers for simultaneous self-regeneration and creation of anticorrosion composite coatings. Andreeva *et al.* applied the deposition of polyelectrolyte multilayer films with opposite charges onto the surfaces of aluminium materials.<sup>102</sup> These polyelectrolyte multilayer LbL coatings effectively inhibited corrosion processes on aluminium surfaces due to their ability to maintain a stable pH level.

### 2.2. Matrix for thermal energy storage

The combination of natural nanocarriers like sepiolite and crystallohydrates represents an affordable and effective nano-scale energy storage system with significant potential for practical use and scalability due to their natural abundance.<sup>103,104</sup> Aqueous crystallohydrate solutions were prepared and various amounts of sepiolite were added resulting in crystallohydrate/sepiolite dispersions with different crystallohydrate contents (50, 60, 70, 80, 90%). These dispersions were then subjected to



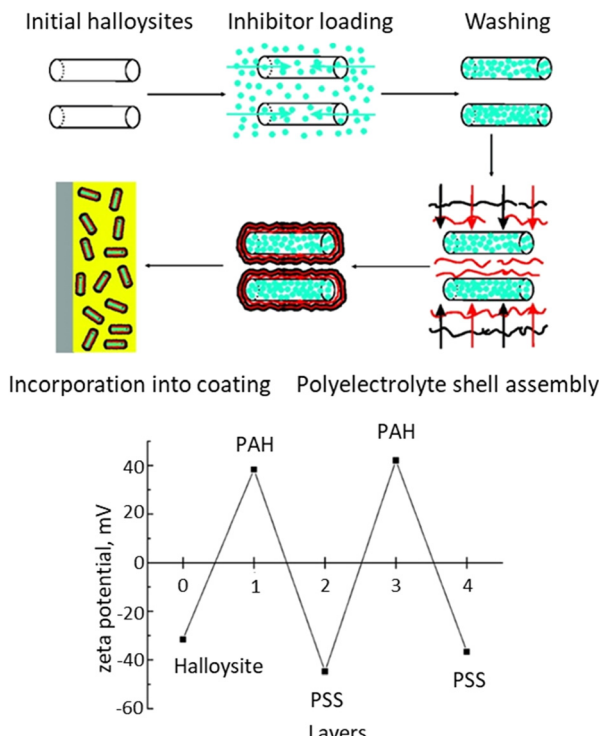


Fig. 2 Synthesis nanocarriers from halloysite loaded with 2-mercaptopbenzothiazole. Zeta potential during polyelectrolyte deposition on halloysite nanotubes at pH 7.5. Reproduced from ref. 101 with permission of publisher. Copyright 2008 American Chemical Society.

ultrasound treatment at 40 °C for 30 minutes, followed by a 10-minute incubation at room temperature. The process was repeated twice to saturate the sepiolite. Composites containing 50%  $\text{Na}_2\text{HPO}_4 \cdot 12\text{H}_2\text{O}$  and 50%  $\text{Na}_2\text{SO}_4 \cdot 10\text{H}_2\text{O}$  demonstrated outstanding thermal energy storage capabilities during heat uptake and release. Sepiolite possesses a unique nanotubular structure, providing a high surface area and demonstrating the ability to accommodate many of hydrated salts. Water molecules and active groups on the sepiolite surface facilitate interactions with these salts.<sup>105,106</sup> Sepiolite-based composites have great potential for thermal energy storage and utilisation, which could be beneficial for temperature regulation in household applications and harnessing low-temperature waste heat.

### 2.3. Nanocontainers for thermal energy storage

Various types of materials are available for thermal energy storage. Solid–liquid phase change materials (PCMs) are among the most promising options due to their high energy density and minimal volume changes during phase transitions. However, ideal PCMs that meet all the necessary criteria, such as high thermal conductivity and safety, have not yet been found. Organic paraffin and crystallohydrates are the most studied, but they also have their drawbacks, such as low thermal conductivity for paraffin and incongruent melting and corrosiveness for crystallohydrates.<sup>76</sup>

The energy properties of solid–liquid PCMs can be enhanced by encapsulating them into micro and nanocontainers.

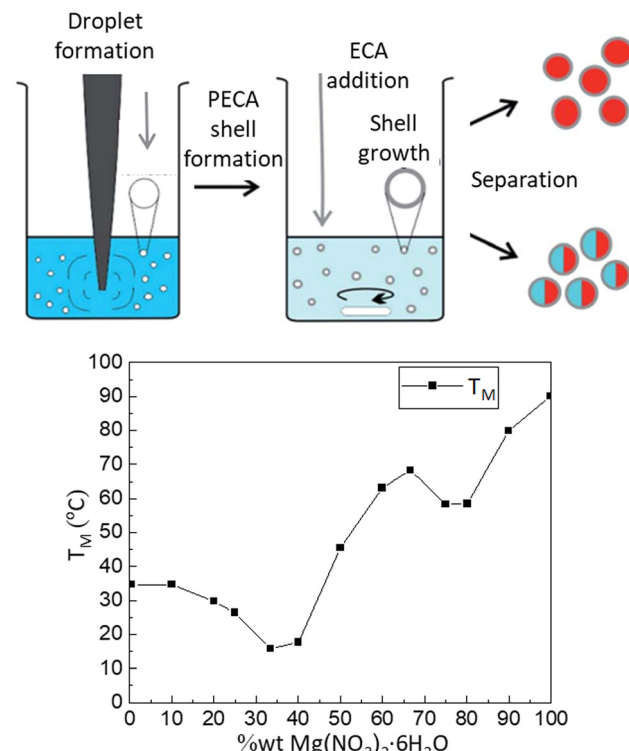


Fig. 3 The process of encapsulating hydrate-loaded capsules: creating a mini-emulsion using ultrasound, forming a PECA shell around the aqueous phase, and the preparation of nanocapsules with either a single or mixed hydrate core. Reproduced from ref. 107 with permission of publisher. Copyright 2017 The Royal Society of Chemistry.

These containers must possess several smart properties, such as controlled release of thermal energy, protection against corrosion and damage, increased contact area with the surrounding environment, and improved thermal conductivity. Energy capsules can thus be used in various bulk systems to impart thermal energy storage properties suitable for practical applications. Graham *et al.*<sup>107</sup> demonstrated a universal method for encapsulating crystallohydrates ( $\text{Mg}(\text{NO}_3)_2 \cdot 6\text{H}_2\text{O}$  and  $\text{Na}_2\text{SO}_4 \cdot 10\text{H}_2\text{O}$ ) and their mixtures into capsules ranging in size from 100 to 300 nm with a poly(ethyl-2-cyanoacrylate), PECA, shell using *in situ* inversion mini-emulsification combined with ultrasound treatment (Fig. 3).

The encapsulated crystallohydrates and their mixtures exhibit high stability during energy storage/release processes (>100 cycles, monitored by differential scanning calorimetry, DSC) due to the functional properties of the capsule shell and spatial confinement preventing water loss and incongruent melting during phase transitions.

### 2.4. Microfluidic synthesis

Polyurethane capsules were synthesised *via* droplets formed inside a microfluidic reactor.<sup>108,109</sup> The capabilities of Dolomite droplet formation are demonstrated in Fig. 4. However, due to the cost of each Dolomite device, it is not worth the risk of polymerisation within. This is where fused deposition modeling (FDM) printed devices would be beneficial in testing in-



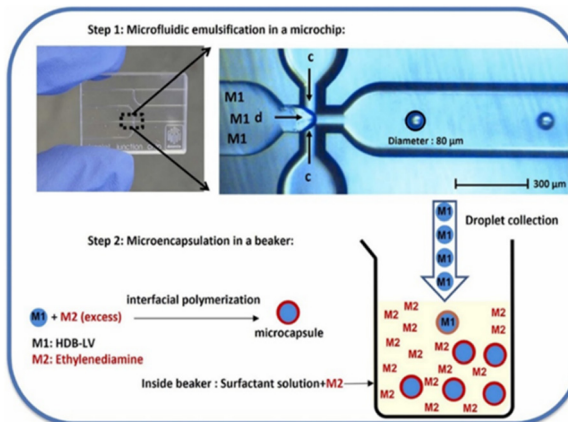


Fig. 4 Microcapsule synthesis via droplet production in a Dolomite device before interfacial polymerisation for shell formation. Reproduced from ref. 110 with the permission of publisher. Copyright 2012, Elsevier.

channel encapsulation.<sup>110</sup> Microencapsulation of calcium chloride hexahydrate in resorcinol resin shell was also demonstrated in a microfluidic reactor.<sup>111</sup> Microcapsules with uniform coating thickness were proved from the optical microscope as well as scanning electron microscope images. DSC results demonstrated that PCM melting in microencapsulated state occurred at a temperature which is within 1 °C from the melting point of bulk PCM. DSC profile after 50 heating/cooling cycles did not show significant changes.

Palazzo *et al.*<sup>112</sup> demonstrated up-scaled encapsulation by supercritical CO<sub>2</sub> emulsification using stearic acid and isopropyl myristate as PCMs in a polymethyl methacrylate (PMMA) shell. Continuous supercritical CO<sub>2</sub> emulsion extraction technology was proposed for the first time to test the encapsulation of stearic acid and isopropyl myristate in PMMA. Spherical microcapsules with smooth surface and average diameter between 163–431 nm were produced. Encapsulation efficiency up to 91% was recorded. Thermograms of the obtained capsules indicated absence of chemical reaction between the core and shell and demonstrated thermal stability for at least 500 heat uptake/release cycles.

### 3. 2D materials for charge storage

The rapid development of technology and the need for more energy have significantly increased the demand for energy storage devices.<sup>113</sup> Flexible supercapacitors (SCs), characterised by a simple manufacturing process, low cost, fast charging, discharge speed and long service life, are particularly interesting among other electrochemical energy storage devices (EES).<sup>114</sup> Due to portability, SCs are easily integrated into wearable sensor devices<sup>115</sup> or different types of EES. The efficiency of supercapacitors is based on the electron/ion transfer and the boundaries/surfaces behaviour during the electrochemical reaction, influencing on the reaction kinetics of the electrode material.<sup>116,117</sup>

Two-dimensional materials are considered innovative and promising candidates for various types of EES with excellent electrical, electrochemical and mechanical properties:

(1) atomic or nanoscale thickness with excellent mechanical properties gives flexibility and durability, which is especially interesting in the development of novel energy storage devices; (2) 2D nanosheets have an ultra-large specific surface area and a better charge distribution, which contributes to the Faraday reaction rate of battery-type electrode materials and improves the storage capacity of capacitor-type electrode materials; (3) the variety of 2D materials allows the development of materials with different chemical compositions and adjustable electrical and electrochemical properties.<sup>118,119</sup> There are many 2D materials with various properties, among which graphene and graphene derivatives are particularly distinguished: graphene oxide (GO), reduced graphene oxide (rGO),<sup>14,120</sup> and graphene nanosheets.<sup>121</sup> The following 2D-material are also widely used: MXenes,<sup>122,123</sup> metal–organic frameworks (MOFs),<sup>124,125</sup> transition metal dichalcogenides (TMDs),<sup>126</sup> covalent organic frameworks (COFs),<sup>127</sup> 2D coordinated polymer.<sup>128</sup>

#### 3.1. Graphene–graphene-based materials

Graphene is a single layer of hexagonally packed carbon atoms. The sp<sup>2</sup>-hybridization of carbon atoms allows delocalising electrons from  $\pi$  bonds, which allows free movement between carbon atoms and creates high electrical conductivity. Graphene also has high specific surface area, extraordinary strength, low density, flexibility and easy chemical processing. These characteristics make graphene and its derivatives ideal materials for electrochemical double-layer capacitor (EDLC) electrodes (Fig. 5). The capacitance characteristics of graphene-based EDLCs depend on several factors, such as specific surface area, pore size distribution, interlayer spacing, heteroatom doping, surface functionality and conductivity.<sup>14,129</sup> Unlike other carbon materials, such as nanotubes, graphene is a strong electrode material due to the strong van der Waals inter-sheet force.<sup>130</sup> However, such a strong attraction contributes to the self-rearrangement of graphene sheets, which decreases the surface area and ion paths for operational charge/discharge.<sup>38,39</sup> Therefore, the actual specific capacity of graphene is lower than the theoretical one.<sup>131</sup> This problem can be solved in two ways: physically increasing the gap between graphene nanosheets and chemical modification of graphene nanosheets to create repulsive forces between them.<sup>132</sup> Various 2D materials can be used as spacers to prevent graphene stacking. According to Wang *et al.*,<sup>132</sup> such spacers should: (1) have a thin and extended 2D network for the physical separation of two adjacent graphene nanosheets; (2) contain mesopores with high porosity to expose graphene surface for ion adsorption/desorption; (3) facilitate the unhindered ion-transportation; and (4) have excellent chemical stability without compromising cycling life. Thus, the formation of rGO/COF hybrids with a COF as a spacer prevented the laying of rGO nanolists and maximised their surface accessibility to electrolyte ions. GO and rGO were used in a similar way to avoid MXenes stacking.<sup>133,134</sup>

#### 3.2. Metal-ion batteries and supercapacitors

For a long time, metal-ion batteries have been widely used worldwide as energy storage devices. There are different types of batteries, depending on the metal.<sup>135</sup> However, lithium-ion



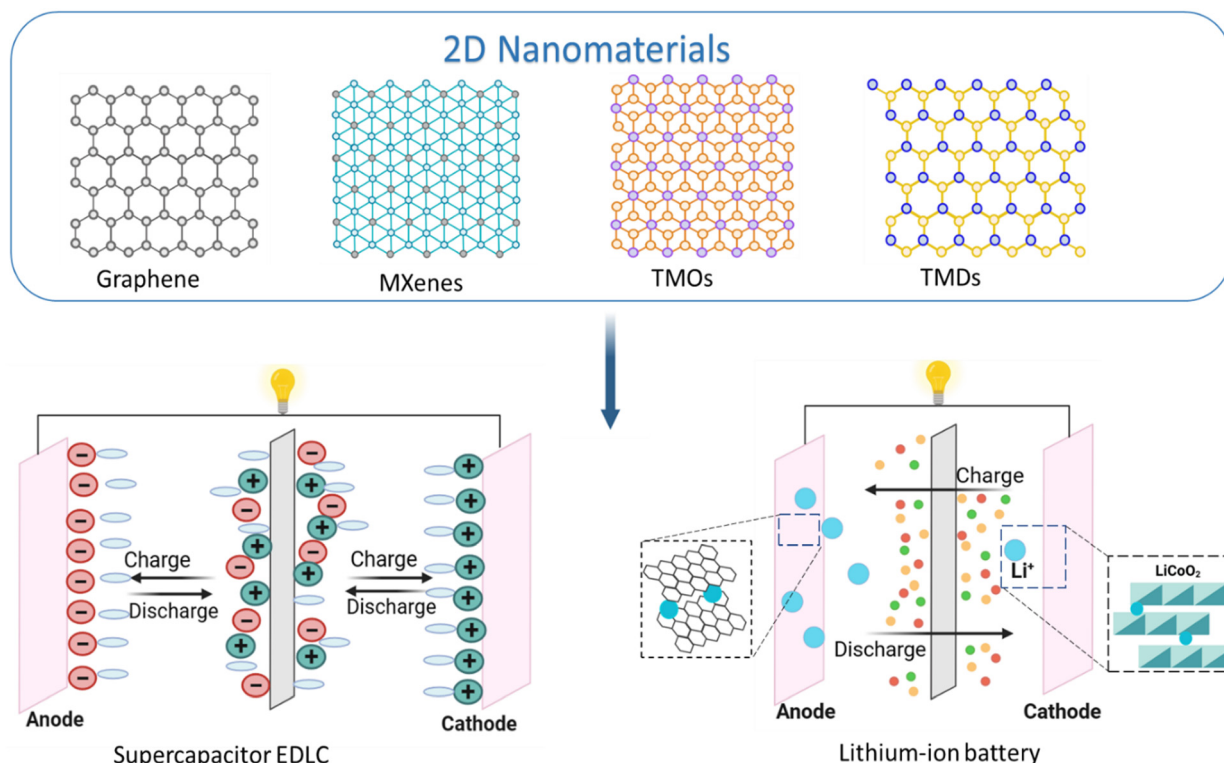


Fig. 5 Various 2D nanomaterials for EDLC and LIB electrode applications.

batteries have become mostly widespread (LIB) (Fig. 5). The characteristics of LIB are mostly influenced by the materials from which the electrodes are made. A traditional lithium-ion battery consists of two electrodes, typically lithium cobalt oxide ( $\text{LiCoO}_2$ ) cathode and graphite ( $\text{C}_6$ ) anode separated by a porous separator immersed in a non-aqueous liquid electrolyte. Li-ions move from the  $\text{LiCoO}_2$  lattice structure to the anode side during charging to form lithiated graphite ( $\text{LiC}_6$ ).<sup>18</sup> Due to the limited storage capacity and moderate diffusion rate of lithium ions in electrode active materials, it is necessary to develop and use new materials to replace existing ones.<sup>136</sup>

Another widespread type of electrochemical energy storage device is supercapacitors.<sup>137</sup> The energy storage mechanism in a supercapacitor originated from the reversible reaction on the surfaces of the electrode materials, which includes charge separation and a faradaic redox reaction at the electrode-electrolyte interface.<sup>138,139</sup> Three types of supercapacitors can be distinguished depending on the mechanism of energy storing: electrical double-layer capacitor (EDLC), pseudocapacitor and hybrid EDLC supercapacitor.<sup>19</sup>

The energy storage process of EDLC (Fig. 5) is based on ion migration. Although the EDLC energy storage mechanism is almost similar to a traditional capacitor and pseudocapacitor, there is an important difference. The mechanism of EDLC does not involve the Faraday redox reaction. Due to this feature, the EDLC is characterised by high stability and charge/discharge rate. However, the EDLC does not have a large specific capacitance like the pseudocapacitor. A hybrid supercapacitor offers electrical double-layer and pseudocapacitor mechanisms

providing high operating potential windows and improved energy densities without compromising power density.<sup>19,140</sup>

### 3.3. Methods of electrode fabrication

Several graphene-based films are prepared for supercapacitors by different methods: vacuum filtration, vacuum-assisted self-assembly, layer-by-layer self-assembly, mechanical compression and solvent evaporation. These methods allow the creation of films with excellent electrical conductivity and the necessary mechanical properties, but they have some disadvantages. Thus, the methods of vacuum filtration, vacuum-assisted self-assembly and mechanical compression require expensive laboratory equipment and are time-consuming. Fabrication of electrode materials by the solvent evaporation method takes 5–10 minutes. It allows the change of the parameters of the film, but there is a possibility of destruction of the film structure by the produced bubbles.<sup>141</sup> Yun *et al.*,<sup>142</sup> the LbL method was used to form layers of rGO and MXene on a wire substrate, which is not easy to do by vacuum filtration. It should also be noted that in comparison with conventional GO membranes prepared by vacuum filtration, multilayer GO membranes assembled by LbL differed in internal structure, wettability and ion permeability.<sup>143</sup>

Special attention should be paid to the combination of graphene-based materials with polyelectrolytes. Due to their electrical conductivity and chemical and mechanical strength, polyelectrolytes are used as materials for EDLCs electrodes in supercapacitors.<sup>144</sup> In addition to these properties, polyelectrolytes can form various structures and layers depending on

parameters such as their molecular weight, pH and ionic strength of the solution.<sup>145</sup> Thus, it is possible to create layers of films with specific parameters using LbL. There are reports discussing the formation of thin films based on graphene nanosheets and graphene-based structures included in a poly-electrolyte matrix of poly(allylamine hydrochloride),<sup>146</sup> poly-aniline,<sup>147</sup> and poly(3,4-ethylenedioxothiophene).<sup>148</sup> Also, Kulandaivalu *et al.*<sup>149</sup> demonstrated polypyrrole (PPy) to form PPy/GO|PPy/MnO<sub>2</sub> layers by LbL. This film improves the electrochemical properties and performance of supercapacitor electrodes by combining the redox reactions of metal oxides with a high surface area/conductivity of graphene. The LbL was successfully used to form rGO/polyelectrolyte films. rGO sheets have a negative charge, due to which they can bind to various polycationic azopolyelectrolytes.<sup>150</sup>

## 4. Application of phase change materials for thermal energy storage

Phase change materials can store thermal energy by undergoing a phase transition, such as from solid to liquid or liquid to gas. PCMs have various applications, including cooling in large areas, regulating temperature fluctuations in buildings or containers, and storing solar energy for short or long periods.<sup>67</sup> When thermal energy comes from periodic sources like solar radiation or waste heat, PCMs offer a compact and efficient way to store and access heat. This section discusses the properties of PCMs improved in combination with 2D materials,<sup>80</sup> focusing on applications for heat storage and solar energy conversion. The safety and sustainability of PCMs are also considered, along with research challenges that need to be addressed for the widespread use of PCMs.<sup>151,152</sup>

### 4.1. PCM composites for controlled heat storage

PCMs can be classified into three main categories based on their chemical nature: organic (o-PCMs), inorganic (io-PCMs) and a combination of both called eutectic (eu-PCMs).<sup>76,153–159</sup> PCMs can also be categorised based on their operating temperature range, latent heat of fusion and energy storage mode. An ideal PCM should have all the necessary characteristics for effective thermal energy storage, but often, a combination of materials is used to achieve the desired properties. The different subgroups of PCMs have a wide range of physical, thermal and chemical properties, which can be used to design thermal energy storage systems.<sup>151,160–163</sup>

Solid-solid PCMs are made of polymer-based materials, such as polyurethanes and polyalcohols. Liquid-gas and gas-solid PCMs are not commonly used because they require large volume and high-pressure systems. Solid-liquid PCMs are the most practical for thermal energy systems. Solid-liquid PCMs absorb heat and behave similarly to the sensible heat storage materials until they reach their phase transition temperature. At this point, they absorb energy without a significant temperature rise and transform into the liquid phase.<sup>152,164,165</sup> PCMs solidify and release the up-taken latent heat when the

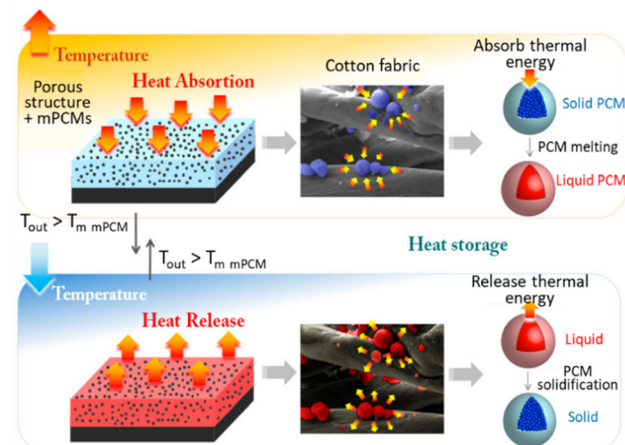


Fig. 6 Microcapsules PCM integrated in cotton fabrics to improve the thermoregulating for commercial applications. Reproduced from ref. 155 with the permission of publisher. Copyright 2012 American Chemical Society.

temperature decreases. o-PCMs, such as paraffin and nonparaffins, have a temperature range of 5–160 °C. io-PCMs, such as salt hydrates and metallic-compounds-based materials, have an effective temperature range of 10–900 °C. Eu-PCMs fall between the temperature ranges of o-PCMs and io-PCMs.<sup>166–168</sup>

In a recent paper,<sup>155</sup> PCMs were developed as microcapsules containing *n*-docosane (Fig. 6). Then, energy capsules were used to impregnate cotton fabrics for thermal energy storage. These fabrics had temperature buffering effect of 11 °C during heating when impregnated with 8 wt% of the microcapsules. They also showed a temperature increase of 6 °C during cooling over 100 cycles of heat uptake/release. This performance was maintained even after storing the fabrics at room temperature for 4 years. In aged fabric composites, the temperature buffering effect during heating increased to 14 °C, and the temperature increase effect during cooling reached 9 °C. The study suggests that microencapsulated *n*-docosane has great potential for thermal management applications in various industries.

### 4.2. 2D materials for solar energy conversion

Utilizing PCM for solar energy storage offers improved energy storage capacity, prolonged heat storage, increased energy conversion efficiency, flexibility in system design and environmental benefits. These advantages make them a promising solution for enhancing the performance and viability of solar energy systems.<sup>169–172</sup> Solar energy storage using PCMs offers a solution to overcome the intermittent nature of solar radiation and enables continuous operation of heating-related processes. Tao *et al.*<sup>173</sup> designed magnetically moving mesh-structured solar absorbers within molten salts to enhance the solar-thermal energy storage rates while maintaining 100% storage capacity. Current storage systems are limited by the low thermal conductivity of PCMs, which hinders their energy-harvesting performance. Presented magnetically movable charging strategy increases the latent heat solar-thermal energy harvesting rate by 107% and supports large-area charging and



batch-to-batch storage. The system can be easily integrated into heat exchanging systems to provide abundant and clean solar-thermal energy for water and space heating.

Shi *et al.*<sup>174</sup> conducted a study of photo-responsive PCM that can store latent heat and photon energy from sunlight. The *ortho*-substitution of azobenzene units allowed photo-switching by irradiation at  $>530$  nm wavelength. Adding an aliphatic group provided a transition between solid and liquid states. The ability to achieve photo-controlled latent heat storage through solar irradiation represents a significant advancement in the field. It opens new avenues for solar energy harvesting utilising functional organic materials, which can be involved in existing systems such as photocatalysts and photovoltaic materials.

Composites based on 2D materials combined with PCM are very effective for solar energy storage. Fan *et al.*<sup>175</sup> developed a new composite PCM based on PEG and  $\text{Ti}_3\text{C}_2\text{T}_x$  nanosheets. The material has high thermal energy storage density. It exhibits strong absorption of electromagnetic waves in the UV-Vis-NIR region due to the localised surface plasmon resonance effect of the  $\text{Ti}_3\text{C}_2\text{T}_x$  nanosheets. As a result, PCM has excellent photo-to-thermal storage efficiency, reaching up to 94.5% under solar light irradiation. Additionally, the composite maintains high energy storage density and remains stable before and after the phase transition. These findings demonstrate that synthesised PCM has superior properties that makes it suitable for solar energy storage applications. PCMs provide a compact and efficient way to store and access heat, especially when the thermal energy comes from intermittent sources like solar radiation or waste heat.<sup>176,177</sup>

## 5. Machine learning for the optimisation of the material

Machine learning (ML) has revolutionized various fields of science and technology, including materials science. Although ML technology appeared in the mid-20th century, its practical use became possible only after the computational power of personal computers significantly increased. ML algorithms require significant computational resources, which allow them to analyze huge volumes of data and identify patterns that would be difficult or impossible for humans to detect. In the field of material optimization, artificial intelligence can accelerate the discovery and development of new materials with desired properties.<sup>178–180</sup> Therefore, many researchers in the field of materials science are interested in how to apply ML methods in their work. Fig. 7a shows growing interest in using machine learning for materials.

Using ML methods, researchers can predict material properties before their synthesis, reducing the time and costs required for experiments. The main advantage of this approach is the minimization of harmful effects during the production of certain materials.<sup>181,182</sup> Therefore, research on machine learning and materials optimization is rapidly developing, especially in the last 10 years, and is already for design of 2D materials,<sup>183–185</sup> hydrogels,<sup>186–189</sup> supramolecular structures,<sup>190</sup> processes of

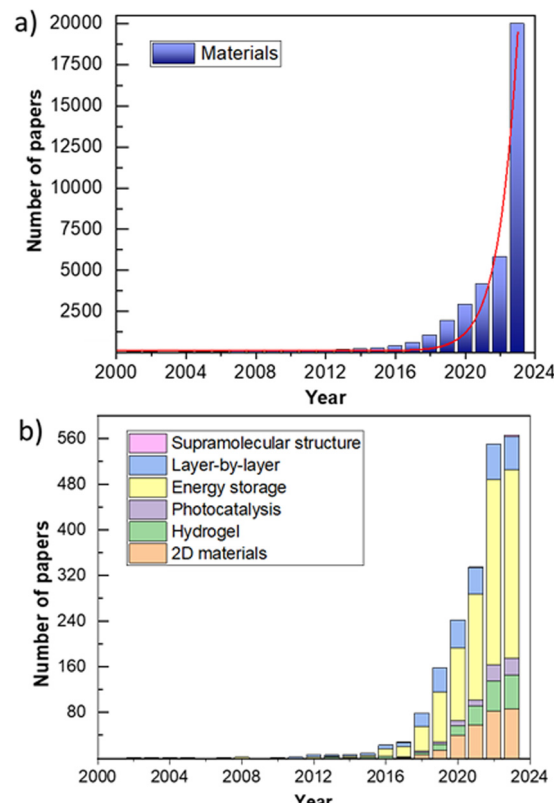


Fig. 7 Histogram of number of scientific publications per year in the Scopus database on the topics (a) machine learning and materials (solid line is an exponential approximation); (b) machine learning and 2D materials/hydrogel/photocatalysis/energy storage/layer-by-layer/supramolecular structure.

photocatalysis,<sup>191–194</sup> energy storage,<sup>195–197</sup> layer-by-layer structures<sup>198,199</sup> and others (Fig. 7b).<sup>200–203</sup>

In this section, we will discuss the current state of applications in optimizing various 2D materials and discuss the problems and opportunities in this rapidly developing field.

### 5.1. ML for 2D-materials

Currently, one of the most important directions in materials science is using machine learning as an effective tool for studying 2D materials for catalysis, energy storage, electronics, optics and biomedical applications. These materials form the basis of modern technologies, and therefore, developing desired properties and changing physical characteristics are important directions. Pure materials are rarely used, and most devices and technologies require careful design of material properties, which can be achieved through doping, creating heterostructures of composites, or controlled introduction of defects. Using computational or experimental data of material properties, machine learning algorithms can predict the structural, electronic, mechanical, and chemical properties of two-dimensional materials that are yet to be discovered. However, to solve such problems, developing an efficient learning model and creating a high-quality database are necessary.

In particular, Novoselov *et al.* demonstrated an approach to revealing the complex correlation between the structure and



properties of defects in 2D materials based on high-throughput data sets.<sup>204</sup> The main task is to compile the correct structured data set to establish and control the structure–property relationships of defects. In the study, the database was compiled using information on the electronic properties of defects obtained from Density Functional Theory calculations in MoS<sub>2</sub> 2D crystals. Defects are often used as a modification tool because they contribute to changes in the properties of solids and, as a result, the properties of 2D materials used in single-atom catalysis. Therefore, it is important to understand the electronic properties of defects in 2D materials. In this study, the distribution of properties of defect configurations was studied by creating a map of the dependence of the forbidden zone on the energy of formation. They also extensively studied the properties of double and triple defects, explaining the variations in properties using symmetry and quantum mechanical analysis of the electronic structure. This study allows for predicting changes in material properties when various defects are introduced by properly organising data and understanding the physics.

## 5.2. Big data analysis by computation methods

In addition to material optimisation tasks, machine learning can analyse large amounts of data. Modern detection methods are important tools for timely fighting various diseases caused by bacteria or viruses. However, many of them take time and require significant resources. In contrast, machine learning algorithms can quickly and accurately analyse large data sets and extract characteristic features, providing a more efficient and economical approach to pathogen detection. Skorb *et al.* demonstrated the use of machine learning for data analysis as a platform for rapid bacterial detection<sup>205</sup> and tick-borne encephalitis detection.<sup>206</sup> This system is based on using a soft hydrogel/eutectic gallium–indium alloy and allows registering nonlinear volt-ampere characteristics depending on the composition of the hydrogel. Hydrogel is a material that has a high water retention capacity and can be used to create an environment conducive to the growth of a pathogenic organisms. ML algorithms were trained on a database collected experimentally by electrochemical characteristics of the system, in particular voltammetric voltage.

Machine learning can also be one of the most effective ways to study and develop new photocatalysts that stimulate further theoretical and experimental research on multicomponent compounds in photocatalytic water splitting. One way to increase the photocatalytic activity of a material is by doping, which involves modifying its optical and electronic properties. Although studies on material doping have been conducted for decades, optimal dopants are still experimentally selected by trial and error. Machine learning can be a promising approach to determining the optimal dopants for high-performance systems by establishing correlations between dopant characteristics and doped materials, which may appear ambiguous when using traditional methods. This reduces the time and costs of experimental research and accelerates the process of discovering new promising materials for use in photocatalytic water

splitting. Wang *et al.* demonstrated a machine learning model predicting changes in the efficiency of photoelectrodes.<sup>207</sup> This work is based on studying changes in the properties of hematite by incorporating 17 different metallic dopants. It was found that when selecting a dopant to improve the material's efficiency, it is necessary to consider the chemical state, ionic radius, and enthalpy of the formation of the metal–oxygen bond. This study demonstrates the possibility of identifying and establishing correlations between dopant characteristics and the properties of doped photoelectrodes, which may be non-obvious for traditional experimental methods.

## 5.3. Usage ML for topological data analysis

Very interesting application for ML is imageanalysis. In recent papers the surface roughness of LbL polyelectrolytes was investigated by using atomic force microscopy.<sup>123,208</sup> The analysis employs innovative techniques such as topological data analysis (TDA) and ML to establish a correlation between multiscale roughness and the number of bilayers as well as to identify the specific type of polyelectrolytes involved. Here researchers compared assemblies polyethyleneimine (PEI)/poly (sodium 4-styrene sulfonate) and PEI/MXene rigid flakes. (Fig. 8)

As the number of bilayers increases, the surface roughness shifts from a smooth profile to an equilibrium roughness. The AFM analysis reveals that the surface morphology exhibits multiscale roughness, with smaller features superimposed on larger ones. To ensure accurate roughness data, various methods are employed, such as correlation length calculations, statistical analysis of extreme values in trimmed images, and the use of TDA barcodes and persistence diagrams in an 8D data space. Additionally, ML algorithm is utilized to determine the number of bilayers in polyelectrolytes. The roughness analysis demonstrates a gradual shift from a smooth to a rough surface, reaching saturation at around three to four bilayers. Moreover, the existence of multiscale roughness invariance is observed.

The use of machine learning for material optimisation has opened up new opportunities for researchers to accelerate the discovery and development of new materials with desired properties. Artificial intelligence can be integrated at any stage of the material design process, depending on the goals set. This

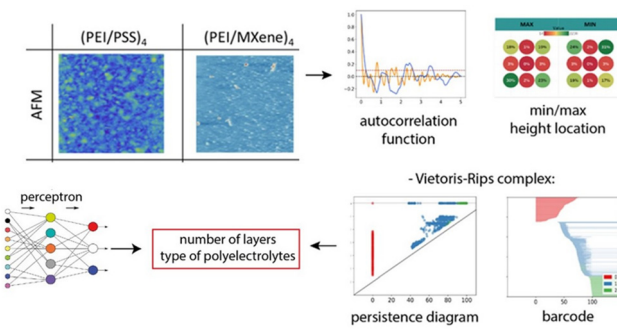


Fig. 8 Schematic representation of the topological data analysis from atomic force microscope images. Reproduced from ref. 209 with the permission of publisher. Copyright 2023 American Chemical Society.



includes the selection of precursors, synthesis parameters, material formation conditions, and their properties. However, some challenges need to be addressed, such as the need for high-quality data and the development of practical machine learning models.

The database for training machine learning algorithms is typically formed using various methods such as experimental data, existing databases, simulations, and modelling. As this field continues to evolve, researchers need to collaborate and share data further to develop the capabilities of machine learning in material optimisation. Thanks to constant innovation and collaboration, the future of materials science with the integration of machine learning methods looks promising. In addition to tasks related to materials optimisation, machine learning can be used as a tool for analysing large volumes of data.

## 6. Conclusions and perspectives

In conclusion, this review highlights the potential of layered materials in the field of renewable energy and explores the use of machine learning techniques to enhance their performance. The following is some potential explorations:

1. 2D materials, such as graphene, transition metal dichalcogenides and black phosphorus, exhibit exceptional properties that make them promising candidates for various renewable energy applications and more. These materials possess high electrical conductivity, excellent mechanical strength, and unique optical properties, enabling their utilization in solar cells, batteries and supercapacitors.

2. The review emphasizes the importance of understanding the structure–property relationships of layered materials to optimize their performance in renewable energy devices. By manipulating the number of layers, doping, and defect engineering, researchers can tailor the properties of these materials to enhance their efficiency, stability, and functionality.

3. Encapsulated or layered PCMs demonstrate significant potential in energy storage applications. Their high surface area, ability to store large amount of heat in small volume and excellent electrical conductivity enable controlled thermal energy storage. The review highlights the advancements in PCMs energy storage systems, including increased energy density, longer cycle life, and faster energy exchange capabilities.

4. Machine learning algorithms offer a powerful tool for predicting and optimizing the properties of 2D materials. Through the application of supervised and unsupervised learning techniques, researchers can efficiently screen a vast number of potential materials, identify their optimal structures, and predict their performance for specific energy-related applications. This approach significantly accelerates the discovery and development of new materials with enhanced efficiency and functionality. Furthermore, the integration of 2D materials with machine learning techniques enables the development of smart energy storage systems. By leveraging the predictive capabilities of machine learning algorithms, researchers can

optimize the charge–discharge behaviour of batteries and supercapacitors based on 2D materials. This leads to improved energy storage capacity, more heat uptake/release cycles, and enhanced overall performance.

In summary, our review demonstrates the immense potential of 2D materials in renewable energy applications. By combining their unique properties with machine learning techniques, researchers can accelerate the discovery of new materials, optimize their performance, and pave the way for the development of more efficient and sustainable energy technologies.

## Author contributions

DGS and EVS were involved in writing original draft, funding acquisition and editing. Other co-authors participated in data curation, analysis and investigation. All co-authors equally contributed to this article.

## Conflicts of interest

There are no conflicts to declare.

## Acknowledgements

Authors acknowledge RSF grant no. 21-13-00403 for the support. We thank the Priority 2030 for infrastructural supported. DGS acknowledges support from Alexander von Humboldt foundation.

## Notes and references

- 1 H. Lu, J. Tournet, K. Dastafkan, Y. Liu, Y. H. Ng, S. K. Karuturi, C. Zhao and Z. Yin, *Chem. Rev.*, 2021, **121**, 10271–10366.
- 2 N. Abas, A. Kalair and N. Khan, *Futures*, 2015, **69**, 31–49.
- 3 S. Schwietzke, O. A. Sherwood, L. M. P. Bruhwiler, J. B. Miller, G. Etiope, E. J. Dlugokencky, S. E. Michel, V. A. Arling, B. H. Vaughn, J. W. C. White and P. P. Tans, *Nature*, 2016, **538**, 88–91.
- 4 D. Welsby, J. Price, S. Pye and P. Ekins, *Nature*, 2021, **597**, 230–234.
- 5 F. Zhang, P. Zhao, M. Niu and J. Maddy, *Int. J. Hydrogen Energy*, 2016, **41**, 14535–14552.
- 6 Priya, P. S. Deora, Y. Verma, R. A. Muhal, C. Goswami and T. Singh, *Mater. Today Proc.*, 2021, **48**, 1178–1184.
- 7 L. Dai, K. Huang, Y. Xia and Z. Xu, *Green Energy Environ.*, 2021, **6**, 193–211.
- 8 P. Carpejani, É. T. de Jesus, B. L. S. Bonfim Catapan, S. E. Gouvea da Costa, E. Pinheiro de Lima, U. Tortato, C. G. Machado and B. K. Richter, *International Business, Trade and Institutional Sustainability*, 2020.
- 9 D. B. Pal and J. M. Jha, *Sustainable and Clean Energy Production Technologies*, 2022.
- 10 F. Yi, H. Ren, J. Shan, X. Sun, D. Wei and Z. Liu, *Chem. Soc. Rev.*, 2018, **47**, 3152–3188.



11 Q. Guo, N. Chen and L. Qu, *Carbon Energy*, 2020, **2**, 54–71.

12 O. A. Moses, L. Gao, H. Zhao, Z. Wang, M. Lawan Adam, Z. Sun, K. Liu, J. Wang, Y. Lu, Z. Yin and X. Yu, *Mater. Today*, 2021, **50**, 116–148.

13 E. Tan, B. L. Li, K. Ariga, C.-T. Lim, S. Garaj and D. T. Leong, *Bioconjug. Chem.*, 2019, **30**, 2287–2299.

14 G. F. Smaisim, A. M. Abed, H. Al-Madhahchi, S. K. Hadrawi, H. M. M. Al-Khateeb and E. Kianfar, *Bionanoscience*, 2023, **13**, 219–248.

15 Y. Tian, Z. Yu, L. Cao, X. L. Zhang, C. Sun and D.-W. Wang, *J. Energy Chem.*, 2021, **55**, 323–344.

16 S. Wang, S. Zhao, X. Guo and G. Wang, *Adv. Energy Mater.*, 2022, **12**, 1–21.

17 X. Tian, Y. Yi, Z. Wu, G. Cheng, S. Zheng, B. Fang, T. Wang, D. G. Shchukin, F. Hai, J. Guo and M. Li, *Chem. Eng. Sci.*, 2023, **266**, 118271.

18 J. Xie and Y.-C. Lu, *Nat. Commun.*, 2020, **11**, 2499.

19 M. Tomy, A. Ambika Rajappan, V. VM and X. Thankappan Suryabai, *Energy Fuels*, 2021, **35**, 19881–19900.

20 W. Zhang, R. Mazzarello, M. Wuttig and E. Ma, *Nat. Rev. Mater.*, 2019, **4**, 150–168.

21 H. Wang, Y. Wang, Z. Ni, N. Turetta, S. M. Gali, H. Peng, Y. Yao, Y. Chen, I. Janica, D. Beljonne, W. Hu, A. Ciesielski and P. Samorì, *Adv. Mater.*, 2021, **33**, 1–9.

22 F. Gao, H. Yang and P. A. Hu, *Small Methods*, 2018, **2**, 1–13.

23 L. Spitthoff, P. R. Shearing and O. S. Burheim, *Energies*, 2021, **14**, 1248.

24 D. V. A. K. Yang, Z. Hu, X. Li, K. Nikolaev, G. K. Hong, N. Mamchik, I. Erofeev, U. M. Mirsaidov, A. H. Castro Neto, D. J. Blackwood, D. G. Shchukin, M. Trushin and K. S. Novoselov, *Proc. Natl. Acad. Sci. U. S. A.*, 2023, **120**, e2307618120.

25 A. T. Press, P. Babic, B. Hoffmann, T. Müller, W. Foo, W. Hauswald, J. Benecke, M. Beretta, Z. Cseresnýs, S. Hoeppener, I. Nischang, S. M. Coldewey, M. H. Gräler, R. Bauer, F. Gonnert, N. Gafslér, R. Wetzker, M. T. Figge, U. S. Schubert and M. Bauer, *EMBO Mol. Med.*, 2021, **13**, e14436.

26 R. M. Nauman Javed, A. Al-Othman, M. Tawalbeh and A. G. Olabi, *Renew. Sustainable Energy Rev.*, 2022, **168**, 112836.

27 O. Okhay and A. Tkach, *Nanomaterials*, 2021, **11**, 1240.

28 F. Farjadian, S. Abbaspour, M. A. A. Sadatlu, S. Mirkiani, A. Ghasemi, M. Hoseini-Ghahfarokhi, N. Mozaffari, M. Karimi and M. R. Hamblin, *ChemistrySelect*, 2020, **5**, 10200–10219.

29 M. Singh, A. Shukla and B. Chakraborty, *Int. J. Hydrogen Energy*, 2022, **1**, 1–14.

30 X. Gao, H. Liu, D. Wang and J. Zhang, *Chem. Soc. Rev.*, 2019, **48**, 908–936.

31 J. Li, Z. Chen, H. Yang, Z. Yi, X. Chen, W. Yao, T. Duan, P. Wu, G. Li and Y. Yi, *Nanomaterials*, 2020, **10**, 257.

32 V. H. Nguyen, T. P. Nguyen, T. H. Le, D. V. N. Vo, D. L. T. Nguyen, Q. T. Trinh, I. T. Kim and Q. Van Le, *J. Chem. Technol. Biotechnol.*, 2020, **95**, 2597–2607.

33 P. Lin, J. Xie, Y. He, X. Lu, W. Li, J. Fang, S. Yan, L. Zhang, X. Sheng and Y. Chen, *Sol. Energy Mater. Sol. Cells*, 2020, **206**, 110229.

34 A. Bhat, S. Anwer, K. S. Bhat, M. I. H. Mohideen, K. Liao and A. Qurashi, *npj 2D Mater. Appl.*, 2021, **5**, 1–21.

35 H. Huang, T. Shi, R. He, J. Wang, P. K. Chu and X. F. Yu, *Adv. Sci.*, 2020, **7**, 1–7.

36 S. Kaushik and R. Singh, *Adv. Opt. Mater.*, 2021, **9**, 1–20.

37 C. Cho, P. Kang, A. Taqieddin, Y. Jing, K. Yong, J. M. Kim, M. F. Haque, N. R. Aluru and S. Nam, *Nat. Electron.*, 2021, **4**, 126–133.

38 H. Hou, C. Anichini, P. Samorì, A. Criado and M. Prato, *Adv. Funct. Mater.*, 2022, **32**, 2207065.

39 X. Xu, Z. Lou, S. Cheng, P. C. Y. Chow, N. Koch and H.-M. Cheng, *Chem.*, 2021, **7**, 2989–3026.

40 S. Noreen, M. B. Tahir, A. Hussain, T. Nawaz, J. U. Rehman, A. Dahshan, M. Alzaid and H. Alrobei, *Int. J. Hydrogen Energy*, 2022, **47**, 1371–1389.

41 K. S. Novoselov, A. K. Geim, S. V. Morozov, D. Jiang, Y. Zhang, S. V. Dubonos, I. V. Grigorieva and A. A. Firsov, *Science*, 2004, **306**, 666–669.

42 C. Yang, H. F. Wang and Q. Xu, *Chem. Res. Chinese Univ.*, 2020, **36**, 10–23.

43 H. Zhang, *ACS Nano*, 2015, **9**, 9451–9469.

44 Q. Cui, Y. Zhong, L. Pan, H. Zhang, Y. Yang, D. Liu, F. Teng, Y. Bando, J. Yao and X. Wang, *Adv. Sci.*, 2018, **5**, 1700902.

45 F. Yi, H. Ren, J. Shan, X. Sun, D. Wei and Z. Liu, *Chem. Soc. Rev.*, 2018, **47**, 3152–3188.

46 C. Li, Q. Cao, F. Wang, Y. Xiao, Y. Li, J.-J. Delaunay and H. Zhu, *Chem. Soc. Rev.*, 2018, **47**, 4981–5037.

47 Z. Xie, Y.-P. Peng, L. Yu, C. Xing, M. Qiu, J. Hu and H. Zhang, *Sol. RRL*, 2020, **4**, 1900400.

48 Z. Xiao, R. Wang, D. Jiang, Z. Qian, Y. Li, K. Yang, Y. Sun, Z. Zeng and F. Wu, *ACS Appl. Energy Mater.*, 2021, **4**, 7440–7461.

49 Y. Zhu, S. Wang, J. Ma, P. Das, S. Zheng and Z.-S. Wu, *Energy Storage Mater.*, 2022, **51**, 500–526.

50 X. Li, Z. Huang, C. E. Shuck, G. Liang, Y. Gogotsi and C. Zhi, *Nat. Rev. Chem.*, 2022, **6**, 389–404.

51 Y. Zhang, Y. Zheng, K. Rui, H. H. Hng, K. Hippalgaonkar, J. Xu, W. Sun, J. Zhu, Q. Yan and W. Huang, *Small*, 2017, **13**, 1700661.

52 Z. Zhang, X. Liu, J. Yu, Y. Hang, Y. Li, Y. Guo, Y. Xu, X. Sun, J. Zhou and W. Guo, *WIREs Comput. Mol. Sci.*, 2016, **6**, 324–350.

53 S. Wu, K. S. Hui and K. N. Hui, *Adv. Sci.*, 2018, **5**, 1700491.

54 M. C. Jenkins and S. Lutz, *ACS Synth. Biol.*, 2021, **10**, 857–869.

55 D. Grigoriev, E. Shchukina and D. G. Shchukin, *Adv. Funct. Mater.*, 2017, **4**, 1600318.

56 S. Eiben, C. Koch, K. Altintoprak, G. Tovar, S. Laschat, I. M. Weiss and C. Wege, *Adv. Drug Delivery Rev.*, 2019, **145**, 96–118.

57 D. Diaz, A. Care and A. Sunna, *Genes*, 2018, **9**, 370.

58 S. Pugh, R. McKenna, I. Halloum and D. R. Nielsen, *Metab. Eng. Commun.*, 2015, **2**, 39–45.

59 C. S. Ramirez-Barria, M. Isaacs, C. Parlett, K. Wilson, A. Guerrero-Ruiz and I. Rodríguez-Ramos, *Catal. Today*, 2020, **357**, 8–14.



60 S. Bera, F. Banerjee and S. K. Samanta, *ChemNanoMat*, 2023, **9**, 1–6.

61 H. Liu, X. Wang and D. Wu, *Appl. Therm. Eng.*, 2018, **134**, 603–614.

62 D. G. Shchukin, *Polym. Chem.*, 2013, **4**, 4871–4877.

63 D. I. Njoku, M. Cui, H. Xiao, B. Shang and Y. Li, *Sci. Rep.*, 2017, 1–15.

64 N. Imoro, V. V. Shilovskikh, P. V. Nesterov, A. A. Timralieva, D. Gets, A. Nebalueva, F. V. Lavrentev, A. S. Novikov, N. D. Kondratyuk, N. D. Orekhov and E. V. Skorb, *ACS Omega*, 2021, **6**, 17267–17275.

65 L. Ma, J. Wang, D. Zhang, Y. Huang, L. Huang, P. Wang, H. Qian, X. Li, H. A. Terryn and J. M. C. Mol, *Chem. Eng. J.*, 2021, **404**, 127118.

66 W. Wang, W. Li, W. Fan, X. Zhang, L. Song and C. Xiong, *Chem. Eng. J.*, 2018, **332**, 658–670.

67 B. Gholipour, *Science*, 2019, **366**, 186–187.

68 A. A. Nikitina, S. A. Ulasevich, I. S. Kassirov, E. A. Bryushkova, E. I. Koshel and E. V. Skorb, *Bioconjug. Chem.*, 2018, **20**, 3793–3799.

69 D. Grigoriev, D. Akcakayiran, M. Schenderlein and D. Shchukin, *Corrosion*, 2014, **70**, 446–463.

70 E. Shchukina and D. G. Shchukin, *Langmuir*, 2019, **35**, 8603–8611.

71 D. G. Shchukin and H. Möhwald, *Small*, 2007, **3**, 926–943.

72 D. Lombardo, M. A. Kiselev, S. Magazù and P. Calandra, *Adv. Condens. Matter. Phys.*, 2015, 1–22.

73 K. A. Zahidah, S. Kakooei, M. C. Ismail and P. Bothi Raja, *Prog. Org. Coat.*, 2017, **111**, 175–185.

74 G. L. Li, H. Möhwald and D. G. Shchukin, *Chem. Soc. Rev.*, 2013, **42**, 3628–3646.

75 E. V. Skorb, D. G. Shchukin, H. Möhwald and D. V. Andreeva, *Nanoscale*, 2010, **2**, 722–727.

76 E. M. Shchukina, M. Graham, Z. Zheng and D. G. Shchukin, *Chem. Soc. Rev.*, 2018, **47**, 4156–4175.

77 N. Brezhneva, A. Nikitina, N. Ryzhkov, A. Klestova, A. V. Vinogradov and E. V. Skorb, *J. Sol-Gel Sci. Technol.*, 2019, **89**, 92–100.

78 V. Y. Yurova, P. I. Zyrianova, P. V. Nesterov, V. V. Goncharov, E. V. Skorb and S. A. Ulasevich, *Catalysts*, 2023, **13**, 993.

79 A. Sharshieva, V. A. Iglin, P. V. Nesterov, O. A. Kuchur, E. Garifullina, E. Hey-Hawkins, S. A. Ulasevich, E. V. Skorb, A. V. Vinogradov and M. I. Morozov, *J. Mater. Chem. B*, 2019, **7**, 6810–6821.

80 K. Ariga, E. Ahn, M. Park and B. Kim, *Chem. – Asian J.*, 2019, 2553–2566.

81 A. S. Ivanov, L. V. Pershina, K. G. Nikolaev and E. V. Skorb, *Macromol. Biosci.*, 2021, **21**, 1–16.

82 A. M. Yola, J. Campbell and D. Volodkin, *Appl. Surf. Sci. Adv.*, 2021, **5**, 100091.

83 A. Arkhangelskiy, D. Maniglio, A. Bucciarelli, V. K. Yadavalli and A. Quaranta, *Adv. Mater. Interfaces*, 2021, **8**, 2100324.

84 A. M. Díez-Pascual and A. Rahdar, *Nanomaterials*, 2022, **12**, 949.

85 C. Xu, A. R. Puente-Santiago, D. Rodríguez-Padrón, M. J. Muñoz-Batista, M. A. Ahsan, J. C. Noveron and R. Luque, *Chem. Soc. Rev.*, 2021, **50**, 4856–4871.

86 S. Zhao, F. Caruso, L. Dahne, G. Decher, B. G. De Geest, J. Fan, N. Feliu, Y. Gogotsi, P. T. Hammond, M. C. Hersam, A. Khademhosseini, N. Kotov, S. Leporatti, Y. Li, F. Lisdat, L. M. Liz-Marzan, S. Moya, P. Mulvaney, A. L. Rogach, S. Roy, D. G. Shchukin, A. G. Skirtach, M. M. Stevens, G. B. Sukhorukov, P. S. Weiss, Z. Yue, D. Zhu and W. J. Parak, *ACS Nano*, 2019, **13**, 6151–6169.

87 J. Lee, D. Kyeong, J. Kim and W. Choi, *Int. J. Heat Mass Transf.*, 2022, **184**, 122344.

88 Q. Fan, L. Wen, R. Dong, X. Hu, J. Ma, W. Zhang, X. Li and G. Carmen, *Appl. Surf. Sci.*, 2023, **638**, 158108.

89 J. Lee, J. Kim, B. Seo, D. Shin, S. Hwang and W. Choi, *Int. J. Heat Mass Transf.*, 2023, **209**, 124067.

90 N. V. Ryzhkov, N. Brezhneva and E. V. Skorb, *Surf. Innov.*, 2019, **7**, 145–167.

91 D. V. Andreeva, M. Trushin, A. Nikitina, M. C. F. Costa, P. V. Cherepanov, M. Holwill, S. Chen, K. Yang, S. W. Chee, U. Mirsaidov, A. H. Castro Neto and K. S. Novoselov, *Nat. Nanotechnol.*, 2020, **16**, 174–180.

92 D. Yu, X. Xiao, C. Shokoohi, Y. Wang, L. Sun, Z. Juan, M. J. Kipper, J. Tang, L. Huang, G. S. Han, H. S. Jung and J. Chen, *Adv. Funct. Mater.*, 2023, **33**, 1–35.

93 Y. Lanchuk, A. Nikitina, N. Brezhneva, S. A. Ulasevich, S. N. Semenov and E. V. Skorb, *ChemCatChem*, 2018, **10**, 1798–1803.

94 N. V. Ryzhkov, N. A. Mamchik and E. V. Skorb, *J. R. Soc., Interface*, 2019, **16**, 20180626.

95 S. A. Ulasevich, N. Brezhneva, Y. Zhukova, H. Möhwald, P. Fratzl, F. H. Schacher, D. V. Sviridov, D. V. Andreeva and E. V. Skorb, *Macromol. Biosci.*, 2016, 1422–1431.

96 B. V. Parakhonskiy, W. J. Parak, D. Volodkin and A. G. Skirtach, *Langmuir*, 2019, **35**, 8574–8583.

97 E. V. Skorb and H. Möhwald, *Adv. Mater.*, 2013, **25**, 5029–5043.

98 Z. Zheng, X. Huang, M. Schenderlein, H. Möhwald, G. K. Xu and D. G. Shchukin, *Nanoscale*, 2015, **7**, 2409–2416.

99 Z. Zheng, M. Schenderlein, X. Huang, N. J. Brownbill, F. Blanc and D. Shchukin, *ACS Appl. Mater. Interfaces*, 2015, **7**, 22756–22766.

100 E. Shchukina, H. Wang and D. G. Shchukin, *Chem. Commun.*, 2019, **55**, 3859–3867.

101 D. G. Shchukin, S. V. Lamaka, K. A. Yasakau, M. L. Zheludkevich, M. G. S. Ferreira and H. Möhwald, *J. Phys. Chem. C*, 2008, **112**, 958–964.

102 D. V. Andreeva, D. Fix, H. Möhwald and D. G. Shchukin, *J. Mater. Chem.*, 2008, **18**, 1738–1740.

103 X. Zhu, V. Vinokurov, D. Kopitsyn and D. G. Shchukin, *ACS Omega*, 2021, **6**, 25828–25834.

104 X. Zhu and D. Shchukin, *Adv. Eng. Mater.*, 2018, **20**, 1800618.

105 Y. Luo, S. Xiong, J. Huang, F. Zhang, C. Li, Y. Min, R. Peng and Y. Liu, *Sol. Energy Mater. Sol. Cells*, 2021, **231**, 111300.

106 G. Tian, G. Han, F. Wang and J. Liang, *Sepiolite nanomaterials: Structure, properties and functional applications*, 2019.



107 M. Graham, J. A. Coca-Clemente, E. Shchukina and D. Shchukin, *J. Mater. Chem. A*, 2017, **5**, 13683–13691.

108 J. Li, M. A. J. Mazumder, H. D. H. Stöver, A. P. Hitchcock and I. M. Shirley, *J. Polym. Sci., Part A: Polym. Chem.*, 2011, **49**, 3038–3047.

109 G. Hao, C. Yu, Y. Chen, X. Liu and Y. Chen, *Int. J. Heat Mass Transf.*, 2022, **190**, 122738.

110 J. Du, N. Ibaseta and P. Guichardon, *Chem. Eng. Res. Des.*, 2022, **182**, 256–272.

111 A. Dey and S. Ganguly, *Therm. Sci. Eng. Prog.*, 2023, **40**, 101776.

112 I. Palazzo and E. Reverchon, *J. Supercrit. Fluids*, 2023, **193**, 105807.

113 S. Koohi-Fayegh and M. A. Rosen, *J. Energy Storage*, 2020, **27**, 101047.

114 Y. Zhang, H. Mei, Y. Cao, X. Yan, J. Yan, H. Gao, H. Luo, S. Wang, X. Jia, L. Kachalova, J. Yang, S. Xue, C. Zhou, L. Wang and Y. Gui, *Coord. Chem. Rev.*, 2021, **438**, 213910.

115 J. Liu, M. Liu, Y. Bai, J. Zhang, H. Liu and W. Zhu, *Sensors*, 2020, **20**, 4009.

116 C. Meng, P. Das, X. Shi, Q. Fu, K. Müllen and Z.-S. Wu, *Small Sci.*, 2021, **1**, 2000076.

117 D. Zhang, J. Lu, C. Pei and S. Ni, *Adv. Energy Mater.*, 2022, **12**, 2103689.

118 D. Zhou, L. Zhao and B. Li, *J. Energy Chem.*, 2021, **62**, 27–42.

119 M. Wu, W. Zheng, X. Hu, F. Zhan, Q. He, H. Wang, Q. Zhang and L. Chen, *Small*, 2022, **18**, 2205101.

120 C. Wang, M. Muni, V. Strauss, A. Borenstein, X. Chang, A. Huang, S. Qu, K. Sung, T. Gilham and R. B. Kaner, *Small*, 2021, **17**, 2006875.

121 D. A. Oliveira, R. A. da Silva, M. O. Orlandi and J. R. Siqueira, *J. Mater. Sci.*, 2022, **57**, 7023–7034.

122 A. Aglikov, O. Volkova, A. Bondar, I. Moskalenko, A. Novikov, E. V. Skorb and E. Smirnov, *Chem. Phys. Chem.*, 2023, e202300187.

123 M. Sychov, A. Eruzin, A. Semenova, P. Katashev, S. Mjakin, M. V. Zhukov, A. Aglikov, M. Nosonovsky and E. V. Skorb, *Langmuir*, 2023, **39**, 12336–12345.

124 A. S. Efimova, P. V. Alekseevskiy, M. V. Timofeeva, Y. A. Kenzhebayeva, A. O. Kuleshova, I. G. Koryakina, D. I. Pavlov, T. S. Sukhikh, A. S. Potapov, S. A. Shipilovskikh, N. Li and V. A. Milichko, *Small Methods*, 2023, 2300752.

125 V. Shrivastav Mansi, B. Gupta, P. Dubey, A. Deep, W. Nogala, V. Shrivastav and S. Sundriyal, *Adv. Colloid Interface Sci.*, 2023, **318**, 102967.

126 S. Ali, S. S. Ahmad Shah, M. Sufyan Javed, T. Najam, A. Parkash, S. Khan, M. A. Bajaber, S. M. M. Eldin, R. A. Tayeb, M. M. Rahman and J. Qi, *Chem. Rec.*, 2023, e202300145.

127 R. Iqbal, G. Yasin, M. Hamza, S. Ibraheem, B. Ullah, A. Saleem, S. Ali, S. Hussain, T. Anh Nguyen, Y. Slimani and R. Pathak, *Coord. Chem. Rev.*, 2021, **447**, 214152.

128 B. Pepió, N. Contreras-Pereda, S. Suárez-García, P. Hayati, S. Benmansour, P. Retailleau, A. Morsali and D. Ruiz-Molina, *Ultrason. Sonochem.*, 2021, **72**, 105425.

129 W. Yang, M. Ni, X. Ren, Y. Tian, N. Li, Y. Su and X. Zhang, *Curr. Opin. Colloid Interface Sci.*, 2015, **20**, 416–428.

130 O. D. Salahdin, H. Sayadi, R. Solanki, R. M. R. Parra, M. Al-Thamir, A. T. Jalil, S. E. Izzat, A. T. Hammid, L. A. B. Arenas and E. Kianfar, *Appl. Phys. A: Mater. Sci. Process.*, 2022, **128**, 703.

131 Y. B. Pottathara, H. R. Tiyyagura, Z. Ahmad and K. K. Sadasivuni, *J. Energy Storage*, 2020, **30**, 101549.

132 C. Wang, F. Liu, J. Chen, Z. Yuan, C. Liu, X. Zhang, M. Xu, L. Wei and Y. Chen, *Energy Storage Mater.*, 2020, **32**, 448–457.

133 K. Nasrin, M. Arunkumar, N. Koushik Kumar, V. Sudharshan, S. Rajasekar, D. Mukhilan, M. Arshad and M. Sathish, *Chem. Eng. J.*, 2023, **474**, 145505.

134 M. Zhao, N. Trainor, C. E. Ren, M. Torelli, B. Anasori and Y. Gogotsi, *Adv. Mater. Technol.*, 2019, **4**, 1800639.

135 Y. Liang, H. Dong, D. Aurbach and Y. Yao, *Nat. Energy*, 2020, **5**, 646–656.

136 Y. Bahari, B. Mortazavi, A. Rajabpour, X. Zhuang and T. Rabczuk, *Energy Storage Mater.*, 2021, **35**, 203–282.

137 W. Tian, A. VahidMohammadi, M. S. Reid, Z. Wang, L. Ouyang, J. Erlandsson, T. Pettersson, L. Wågberg, M. Beidaghi and M. M. Hamedi, *Adv. Mater.*, 2019, **31**, 1902977.

138 X. Lang, A. Hirata, T. Fujita and M. Chen, *Nat. Nanotechnol.*, 2011, **6**, 232–236.

139 M. Salanne, B. Rotenberg, K. Naoi, K. Kaneko, P.-L. Taberna, C. P. Grey, B. Dunn and P. Simon, *Nat. Energy*, 2016, **1**, 16070.

140 Q. Zhu, J. Li, P. Simon and B. Xu, *Energy Storage Mater.*, 2021, **35**, 630–660.

141 S. Zhao, M. Li, X. Wu, S. H. Yu, W. Zhang, J. Luo, J. Wang, Y. Geng, Q. Gou and K. Sun, *Mater. Today Adv.*, 2020, **6**, 100060.

142 J. Yun, I. Echols, P. Flouda, Y. Chen, S. Wang, X. Zhao, D. Holta, M. Radovic, M. J. Green, M. Naraghi and J. L. Lutkenhaus, *ACS Appl. Mater. Interfaces*, 2021, **13**, 14068–14076.

143 E. Ahn, H. Gaiji, T. Kim, M. Abderrabba, H.-W. Lee and B.-S. Kim, *J. Memb. Sci.*, 2019, **585**, 191–198.

144 S. Bashir, K. Hasan, M. Hina, R. Ali Soomro, M. A. Mujtaba, S. Ramesh, K. Ramesh, N. Duraisamy and R. Manikam, *J. Electroanal. Chem.*, 2021, **898**, 115626.

145 E. V. Lengert, S. I. Koltsov, J. Li, A. V. Ermakov, B. V. Parakhonskiy, E. V. Skorb and A. G. Skirtach, *Coatings*, 2020, **10**, 1131.

146 D. A. Oliveira, J. L. Lutkenhaus and J. R. Siqueira, *Thin Solid Films*, 2021, **718**, 138483.

147 F. Balqis, B. Prakoso, N. Hanif Hawari, C. Eldona and A. Sumboja, *ChemNanoMat*, 2022, **8**, e202200151.

148 O. Faruk and B. Adak, *Synth. Met.*, 2023, **297**, 117384.

149 S. Kulandaivalu, N. Suhaimi and Y. Sulaiman, *Sci. Rep.*, 2019, **9**, 4884.

150 X.-W. Yun, B. Tang, Z.-Y. Xiong and X.-G. Wang, *Chinese J. Polym. Sci.*, 2020, **38**, 423–434.

151 A. S. Yang, T. Y. Cai, L. Su, Y. S. Li, F. F. He, Q. P. Zhang, Y. L. Zhou, R. He, K. Zhang and W. Bin Yang, *Sustainable Energy Fuels*, 2022, **6**, 5045–5071.



152 K. Shportko, S. Kremers, M. Woda, D. Lencer, J. Robertson and M. Wuttig, *Nat. Mater.*, 2008, **7**, 653–658.

153 D. V. Voronin, R. I. Mendgaziev, M. I. Rubtsova, K. A. Cherednichenko, P. A. Demina, A. M. Abramova, D. G. Shchukin and V. Vinokurov, *Mater. Chem. Front.*, 2022, **6**, 1033–1045.

154 W. Aftab, X. Huang, W. Wu, Z. Liang, A. Mahmood and R. Zou, *Energy Environ. Sci.*, 2018, **11**, 1392–1424.

155 P. F. De Castro, S. Minko, V. Vinokurov, K. Cherednichenko and D. G. Shchukin, *ACS Appl. Energy Mater.*, 2021, **4**, 12789–12797.

156 Q. Qin, W. Cao, D. W. Zhaxi, X. Chen, D. V. Andreeva, K. Chen, S. Yang, H. Tian, M. Shaker, Z. Jin and K. S. Novoselov, *J. Mater. Eng. Perform.*, 2023, **1**, 1–12.

157 M. Wieckowski and M. Krolkowski, *J. Chem. Eng. Data*, 2022, **67**, 727–738.

158 L. Abdolmaleki, S. M. Sadrameli and A. Pirvaram, *Renew. Energy*, 2020, **145**, 233–241.

159 M. Więckowski, M. Królikowski, L. Scheller and M. Dzida, *Phys. Chem. Chem. Phys.*, 2023, **25**, 16979–16990.

160 W. Xu, L. Xu, W. Jia, X. Mao, S. Liu, H. Dong, H. Zhang and Y. Zhang, *Biomater. Sci.*, 2022, **10**, 6388–6398.

161 B. Nie, A. Palacios, B. Zou, J. Liu, T. Zhang and Y. Li, *Renew. Sustainable Energy Rev.*, 2020, **134**, 513–533.

162 S. Amin, Z. Ma and M. Arici, *Building Energy Flexibility and Demand Management*, 2023.

163 Y. Feng, R. Wei, Z. Huang, X. Zhang and G. Wang, *Phys. Chem. Chem. Phys.*, 2018, **20**, 7772–7780.

164 M. Zhu, O. Cojocaru-mirédin, A. M. Mio, J. Keutgen, M. Küpers, Y. Yu, J. Cho, R. Dronskowski and M. Wuttig, *Adv. Mater.*, 2018, **30**, 1706735.

165 N. Ravikiran, B. Padya, A. Rao, R. Kali and P. K. Jain, *Multifunct. Phase Chang. Mater. Fundam. Prop. Appl.*, 2023, 95–112.

166 K. Du, J. Calautit, Z. Wang, Y. Wu and H. Liu, *Appl. Energy*, 2018, **220**, 242–273.

167 V. Kulish, N. Aslfattahi, M. Schmirler and P. Sláma, *Sci. Rep.*, 2023, 1–12.

168 S. Fatahi, H. Claverie and J. Poncet, *Appl. Sci.*, 2022, **12**, 12019.

169 K. Matuszek, M. Kar, J. M. Pringle and D. R. Macfarlane, *Chem. Rev.*, 2023, **123**, 491–514.

170 Y. Zhang, J. Tang, J. Chen, Y. Zhang, X. Chen, M. Ding, W. Zhou, X. Xu, H. Liu and G. Xue, *Nat. Commun.*, 2023, **14**, 1–10.

171 H. Cho, J. Kwon, I. Ha, J. Jung, Y. Rho, H. Lee, S. Han, S. Hong, C. P. Grigoropoulos and S. H. Ko, *Sci. Adv.*, 2019, **5**, 1–9.

172 S. S. Mali, J. V. Patil, J. Y. Shao, Y. W. Zhong, S. R. Rondiya, N. Y. Dzade and C. K. Hong, *Nat. Energy*, 2023, **8**, 1–13.

173 P. Tao, C. Chang, Z. Tong, H. Bao, C. Song, J. Wu, W. Shang and T. Deng, *Energy Environ. Sci.*, 2019, **12**, 1613–1621.

174 Y. Shi, M. A. Gerkman, Q. Qiu, S. Zhang and G. G. D. Han, *J. Mater. Chem. A*, 2021, **9**, 9798–9808.

175 X. Fan, L. Liu, X. Jin, W. Wang, S. Zhang and B. Tang, *J. Mater. Chem. A*, 2019, **7**, 14319–14327.

176 B. Gupta, J. Bhalavi, S. Sharma and A. Bisen, *Mater. Today Proc.*, 2020, **46**, 5550–5554.

177 V. Chalkia, N. Tachos, P. K. Pandis, A. Giannakas, M. K. Koukou, M. G. Vrachopoulos, L. Coelho, A. Ladavos and V. N. Stathopoulos, *RSC Adv.*, 2018, **8**, 27438–27447.

178 A. S. Rosen, S. M. Iyer, D. Ray, Z. Yao, A. Aspuru-Guzik, L. Gagliardi, J. M. Notestein and R. Q. Snurr, *Matter*, 2021, **4**, 1578–1597.

179 Z. Yao, B. Sánchez-Lengeling, N. S. Bobbitt, B. J. Bucior, S. G. H. Kumar, S. P. Collins, T. Burns, T. K. Woo, O. K. Farha, R. Q. Snurr and A. Aspuru-Guzik, *Nat. Mach. Intell.*, 2021, **3**, 76–86.

180 G. Pilania, J. E. Gubernatis and T. Lookman, *Comput. Mater. Sci.*, 2017, **129**, 156–163.

181 C. Gao, X. Min, M. Fang, T. Tao, X. Zheng, Y. Liu, X. Wu and Z. Huang, *Adv. Funct. Mater.*, 2022, **32**, 2108044.

182 C. Liu, E. Fujita, Y. Katsura, Y. Inada, A. Ishikawa, R. Tamura, K. Kimura and R. Yoshida, *Adv. Mater.*, 2021, **33**, 2102507.

183 H. Ning, Z. Yu, Q. Zhang, H. Wen, B. Gao, Y. Mao, Y. Li, Y. Zhou, Y. Zhou, J. Chen, L. Liu, W. Wang, T. Li, Y. Li, W. Meng, W. Li, Y. Li, H. Qiu, Y. Shi, Y. Chai, H. Wu and X. Wang, *Nat. Nanotechnol.*, 2023, **18**, 493–500.

184 S. Wu, Z. Wang, H. Zhang, J. Cai and J. Li, *Energy Environ. Mater.*, 2023, **6**, e12259.

185 H. J. Kim, M. Chong, T. G. Rhee, Y. G. Khim, M.-H. Jung, Y.-M. Kim, H. Y. Jeong, B. K. Choi and Y. J. Chang, *Nano Converg.*, 2023, **10**, 10.

186 M. Seifermann, P. Reiser, P. Friederich and P. A. Levkin, *Small Methods*, 2023, **7**, 2300553.

187 T. Xu, J. Wang, S. Zhao, D. Chen, H. Zhang, Y. Fang, N. Kong, Z. Zhou, W. Li and H. Wang, *Nat. Commun.*, 2023, **14**, 3880.

188 N. Madadian Bozorg, M. Leclercq, T. Lescot, M. Bazin, N. Gaudreault, A. Dikpati, M.-A. Fortin, A. Droit and N. Bertrand, *Biomater. Adv.*, 2023, **153**, 213533.

189 J. Zhang, Y. Liu, D. Chandra Sekhar, M. Singh, Y. Tong, E. Kucukdeger, H. Y. Yoon, A. P. Haring, M. Roman, Z. (James) Kong and B. N. Johnson, *Appl. Mater. Today*, 2023, **30**, 101720.

190 E. Vargo, J. C. Dahl, K. M. Evans, T. Khan, P. Alivisatos and T. Xu, *Adv. Mater.*, 2022, **34**, 2203168.

191 Z. H. Jaffari, A. Abbas, S.-M. Lam, S. Park, K. Chon, E.-S. Kim and K. H. Cho, *J. Hazard. Mater.*, 2023, **442**, 130031.

192 Z. Zhao, Y. Shen, H. Zhu, Q. Zhang, Y. Zhang, X. Yang, P. Liang and L. Chen, *Appl. Surf. Sci.*, 2023, **640**, 158400.

193 A. Esmaili, S. Pourranjabar Hasan Kiadeh, A. Ebrahimian Pirbazari, F. Esmaili Khalil Saraei, A. Ebrahimian Pirbazari, A. Derakhshesh and F.-S. Tabatabai-Yazdi, *Chemosphere*, 2023, **332**, 138852.

194 J. Li, X. Liu, H. Wang, Y. Sun and F. Dong, *Chinese Chem. Lett.*, 2023, 108596.

195 T. Lemaoui, A. S. Darwish, G. Almustafa, A. Boublia, P. R. Sarika, N. A. Jabbar, T. Ibrahim, P. Nancarrow, K. K. Yadav, A. M. Fallatah, M. Abbas, J. S. Algethami, Y. Benguerba, B.-H. Jeon, F. Banat and I. M. AlNashef, *Energy Storage Mater.*, 2023, **59**, 102795.



196 H. Yang, L. Fang, Z. Yuan, X. Teng, H. Qin, Z. He, Y. Wan, X. Wu, Y. Zhang, L. Guan, C. Meng, Q. Zhou, C. Wang, P. Ding, H. Hu and M. Wu, *Carbon*, 2023, **201**, 408–414.

197 Y. Zhang and M. Zhao, *Energy Storage Mater.*, 2023, **57**, 346–359.

198 T. Šušteršič, V. Gribova, M. Nikolic, P. Lavalle, N. Filipovic and N. E. Vrana, *ACS Omega*, 2023, **8**, 4677–4686.

199 L. Pilz, C. Natzeck, J. Wohlgemuth, N. Scheuermann, P. G. Weidler, I. Wagner, C. Wöll and M. Tsotsalas, *Adv. Mater. Interfaces*, 2023, **10**, 2201771.

200 E. E. Ondar, M. V. Polynski and V. P. Ananikov, *Chem-PhysChem*, 2023, **24**, e202200940.

201 D. A. Boiko, K. S. Kozlov, J. V. Burykina, V. V. Ilyushenkova and V. P. Ananikov, *J. Am. Chem. Soc.*, 2022, **144**, 14590–14606.

202 J. Razlivina, N. Serov, O. Shapovalova and V. Vinogradov, *Small*, 2022, **18**, 2105673.

203 N. Shirokii, Y. Din, I. Petrov, Y. Seregin, S. Sirotenko, J. Razlivina, N. Serov and V. Vinogradov, *Small*, 2023, **19**, 2207106.

204 P. Huang, R. Lukin, M. Faleev, N. Kazeev, A. R. Al-Maeeni, D. V. Andreeva, A. Ustyuzhanin, A. Tomasov, A. H. Castro Neto and K. S. Novoselov, *npj 2D Mater. Appl.*, 2023, **7**, 6.

205 F. V. Lavrentev, I. S. Rumyantsev, A. S. Ivanov, V. V. Shilovskikh, O. Y. Orlova, K. G. Nikolaev, D. V. Andreeva and E. V. Skorb, *ACS Appl. Mater. Interfaces*, 2022, **14**, 7321–7328.

206 A. S. Ivanov, K. G. Nikolaev, A. A. Stekolshchikova, W. T. Tesfatsion, S. O. Yurchenko, K. S. Novoselov, D. V. Andreeva, M. Y. Rubtsova, M. F. Vorovitch, A. A. Ishmukhametov, A. M. Egorov and E. V. Skorb, *ACS Appl. Bio Mater.*, 2020, **3**, 7352–7356.

207 Z. Wang, Y. Gu, L. Zheng, J. Hou, H. Zheng, S. Sun and L. Wang, *Adv. Mater.*, 2022, **34**, 2106776.

208 M. Zhukov, M. S. Hasan, P. Nesterov, M. Sabbouh, O. Burdulenko, E. V. Skorb and M. Nosonovsky, *ACS Appl. Mater. Interfaces*, 2022, **14**, 2351–2359.

209 A. S. Aglikov, A. T. Aliev, M. V. Zhukov, A. A. Nikitina, E. A. Smirnov, D. A. Kozodaev, M. I. Nosonovsky and E. V. Skorb, *ACS Appl. Electr. Mater.*, 2023, DOI: [10.1021/acsaem.3c01358](https://doi.org/10.1021/acsaem.3c01358).

